

# Journal of Biomedical Optics

[SPIDigitalLibrary.org/jbo](http://SPIDigitalLibrary.org/jbo)

## Photoacoustic microscopy of blood pulse wave

Chenghung Yeh  
Song Hu  
Konstantin Maslov  
Lihong V. Wang

# Photoacoustic microscopy of blood pulse wave

Chenghung Yeh,\* Song Hu,\* Konstantin Maslov, and Lihong V. Wang

Washington University in St. Louis, Optical Imaging Laboratory, Department of Biomedical Engineering, One Brookings Drive, St. Louis, Missouri 63130-4899

**Abstract.** Blood pulse wave velocity (PWV) is an important physiological parameter that characterizes vascular stiffness. In this letter, we present electrocardiogram-synchronized, photoacoustic microscopy for noninvasive quantification of the PWV in the peripheral vessels of living mice. Interestingly, blood pulse wave-induced fluctuations in blood flow speed were clearly observed in arteries and arterioles, but not in veins or venules. Simultaneously recorded electrocardiograms served as references to measure the travel time of the pulse wave between two cross sections of a chosen vessel and vessel segmentation analysis enabled accurate quantification of the travel distance. PWVs were quantified in ten vessel segments from two mice. Statistical analysis shows a linear correlation between the PWV and the vessel diameter which agrees with known physiology. © 2012 Society of Photo-Optical Instrumentation Engineers (SPIE). [DOI: 10.1117/1.JBO.17.7.070504]

Keywords: optical-resolution photoacoustic microscopy; electrocardiography; pulse wave velocity.

Paper 12248L received Apr. 20, 2012; revised manuscript received May 22, 2012; accepted for publication May 22, 2012; published online Jun. 28, 2012.

Cardiovascular diseases, particularly hypertension and atherosclerosis, often induce pathological changes to arterial compliance and resistance.<sup>1,2</sup> Consequent pathological change in local blood pulse wave velocity (PWV) has been widely adopted as a robust disease indicator.<sup>2,3</sup> Traditional Doppler ultrasound has been used for PWV measurements, however, it is limited to large trunk vessels.<sup>1,4,5</sup>

Photoacoustic microscopy (PAM) is capable of high sensitivity, high resolution, and noninvasive vascular imaging *in vivo*,<sup>6</sup> extending PWV measurements to small peripheral vessels. In this letter, by simultaneously monitoring blood flow speed and cardiac pulsation using a combined PAM-electrocardiography (ECG) system, we demonstrated the first *in vivo* photoacoustic measurement of the PWV in the mouse peripheral vasculature.

The dual-modal system consists of a second-generation optical-resolution PAM (OR-PAM) system<sup>7</sup> and a home-made ECG recorder, as seen in Fig. 1. In OR-PAM, the outputs of a solid-state laser (SPOT, Elforlight) and a wavelength-tunable laser system (pump laser: INNOSLAB, Edgewave; dye laser:

CBR-D, Sirah) were combined using a beam splitter to provide pulse-to-pulse wavelength switching for the measurement of hemoglobin oxygen saturation (SO<sub>2</sub>). The combined laser beam was spatially filtered by an iris (ID25SS, Thorlabs; aperture size: 2 mm), focused by a condenser lens (LA1131, Thorlabs) through a 50- $\mu$ m-diameter pinhole (P50C, Thorlabs), and then coupled into a single-mode fiber (PA-460A-FC-2, Thorlabs). A tunable neutral density filter (NDC-50C-2M, Thorlabs) was placed before the fiber coupler to regulate the intensity of the incident beam. The fiber output was collimated by a microscope objective (RMS4X, Thorlabs), reflected by a mirror, and re-focused by a second identical objective to achieve nearly diffraction-limited optical focusing (focal diameter: 2.6  $\mu$ m). A home-made acoustic-optical beam combiner, containing an oil-filled interface, was placed beneath the objective to align the optical excitation and ultrasound detection coaxially and confocally. The generated photoacoustic wave was focused by an acoustic lens, detected by an unfocused ultrasonic transducer (V214-BB-RM, Olympus-NDT), and amplified by two 24-dB cascaded electrical amplifiers (ZFL 500LN, Mini-Circuits). Electrocardiograms were simultaneously recorded with three electrodes, one connected to the ground, one to a front leg, and one to a hind leg of a mouse. The ECG signals were then amplified by a high-gain differential amplifier (Model 3000, A-M systems). The acquired photoacoustic and ECG signals were digitized by a dual-channel high-resolution digitizer (NI PCI 5124, National Instruments Corporation) and stored in a computer for offline data processing.

To study the differential responses of arteries and veins to the cardiac pulsation, we identified the major arteries and veins, in a 5  $\times$  2.5 mm<sup>2</sup> region of interest in a mouse ear, using a dual-wavelength OR-PAM measurement (532 nm from the SPOT laser and 563 nm from the Sirah laser), as seen in Fig. 2(a). Then, two cross sections, one from an artery and one from a vein and depicted by arrows in Fig. 2(a), were selected for a 30-second OR-PAM monitoring of the blood flow during which an electrocardiogram was simultaneously recorded. Figure 2(b) and 2(c) showed representative one-second segments of the recorded blood flow and ECG patterns in the artery and vein, respectively. Fourier analysis of the entire 30-second blood flow pattern and electrocardiogram showed a strong pulsation-induced oscillation tone in the arterial blood flow, as seen in Fig. 3(d), but not the venous flow, as shown in Fig. 3(e), which is consistent with previously reported observations.<sup>4</sup> Physiologically speaking,<sup>8</sup> arterial blood is actively transported by the beating of the heart. In contrast, the transportation of venous blood is passively regulated by valves and driven by the skeletal-muscle neither have a correlation with heart beat. Therefore, we focused on PWV measurements in peripheral arteries and arterioles.

By definition, PWV is the distance traveled,  $\Delta l$ , by the blood pulse wave divided by the corresponding travel time,  $\Delta t$ . Ideally, to measure  $\Delta t$ , the blood flow patterns at both the starting and ending points of the travel path should be recorded simultaneously. However, our current OR-PAM system is based on focused scanning, which allows flow patterns to be monitored at only one location at a time.

To solve this problem, we simultaneously recorded ECG signals as references, a technique previously adopted for ultrasound-based PWV measurements.<sup>9</sup> As shown in Fig. 3(a),

\*Authors contributed equally to this work.

Address all correspondence to: Lihong V. Wang, Optical Imaging Laboratory, Department of Biomedical Engineering, Washington University in St. Louis, One Brookings Drive, St. Louis, Missouri 63130-4899. Tel: +1 (314) 935-6152; Fax: +1 (314) 935-7448; E-mail: [lhwang@wustl.edu](mailto:lhwang@wustl.edu)

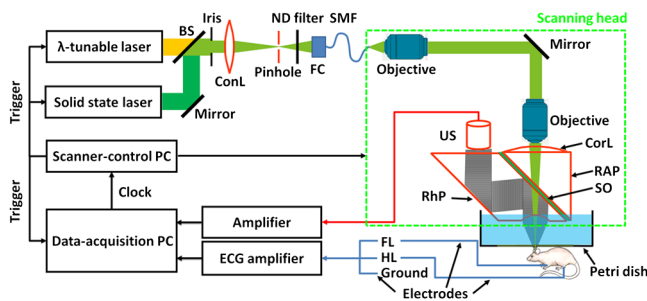


**Fig. 1** Schematic of the ECG-synchronized OR-PAM system for PWV measurement.  $\lambda$ , wavelength; BS, beam splitter; ConL, condenser lens; ND, neutral density; FC, fiber collimator; SMF, single-mode fiber; CorL, correction lens; RAP, right-angle prism; SO, silicone oil; RhP, rhomboid prism; US, ultrasonic transducer; FL, foreleg; HL, hind leg; PC, personal computer.

the ECG and blood flow patterns were divided into single-period segments according to the R-spike of the ECG signal in each cardiac cycle. Then, all the single-period segments of the flow patterns, indicated by the thin blue curves in Fig. 3(b), were aligned according to their corresponding ECG R-spikes to compute an average, which is depicted by the thick black curve in Fig. 3(b). For more accurate quantification of  $\Delta t$ ,

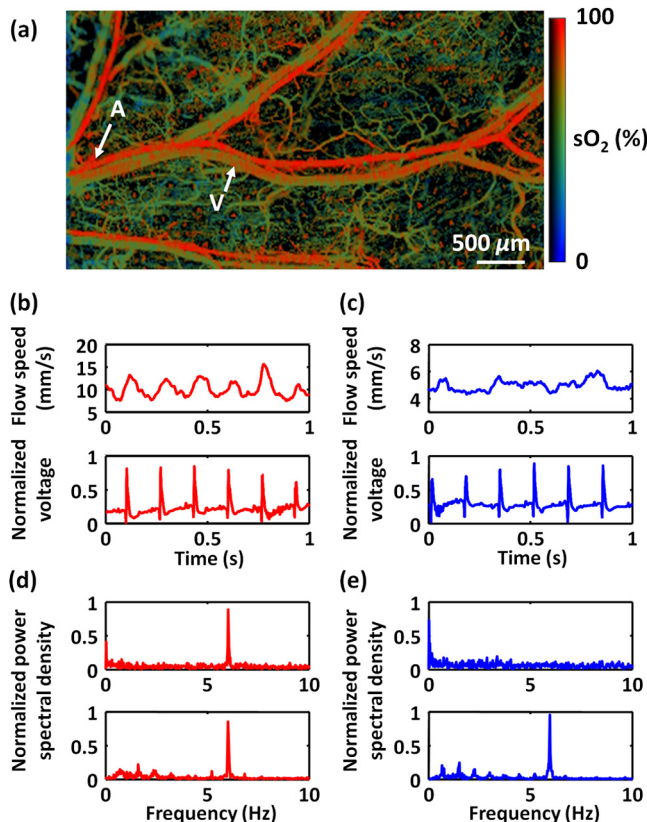


**Fig. 2** Differential responses of artery and vein to cardiac pulsation. (a) Dual-wavelength (532 nm and 563 nm) OR-PAM of  $SO_2$  in a nude mouse ear. A, a cross section in the artery; V, a cross section in the vein. (b) Simultaneous measurements of the arterial flow speed at cross section; A (top) and ECG (bottom). (c) Simultaneous measurements of the venous flow speed at cross section V (top) and ECG (bottom). (d) Normalized power spectra of the arterial flow speed (top) and ECG (bottom) signals shown in (b). (e) Normalized power spectra of the venous flow speed (top) and ECG (bottom) signals shown in (c).

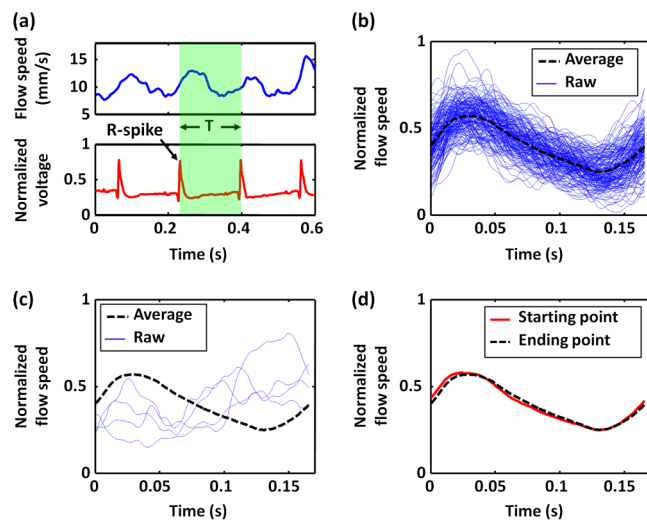


**Fig. 3** Four-step procedure for PWV quantification. (a) Simultaneously recorded blood flow patterns and ECG are divided into single-period segments according to the R-spike of the ECG signal in each cardiac cycle. (b) The single-period raw flow segments are aligned according to the ECG R-spikes and then averaged. (c) The average flow pattern is correlated with the raw flow pattern in each period, and the outliers with negative correlations are discarded. (d) The average flow patterns acquired at the starting and ending points of the travel path are aligned according to their ECG counterparts, and the travel time of the pulse wave is computed using cross-covariance.

the average was correlated with the raw flow pattern in each period and those with poor cross-covariance, cross-covariance coefficient  $< 0$ , were discarded, as indicated by the thin blue curves in Fig. 3(c). The remaining raw single-period flow patterns were re-averaged over all periods. The average flow patterns acquired at the starting, shown by the red solid curve in Fig. 3(d), and ending, indicated by the black dashed curve in Fig. 3(d), points of the travel path were compared to compute  $\Delta t$  using cross-covariance. Furthermore, the travel distance,  $\Delta l$ , was measured along the vessel axis using vessel segmentation analysis.<sup>10</sup> With experimentally measured  $\Delta l$  and  $\Delta t$ , the PWV was computed by taking the ratio.

Given the limited temporal resolution of 0.65 ms in our current measurement of blood flow, a  $\Delta l$  of  $\sim 1$  mm was preferred to ensure that a PWV of up to 160 cm/s can be measured. However,  $\Delta l$  should never exceed the vascular length between two adjacent bifurcation points because vascular bifurcation might induce abrupt changes to the phase of the pulse wave. Increasing  $\Delta l$  can further extend the maximum measurable PWV, at the expense of localizability. Alternatively, higher repetition-rate pulsed lasers can improve the temporal resolution, thereby, enhancing the measurability of a large PWV without sacrificing the localizability. The minimum measurable PWV is determined by the minimum  $\Delta l$  and maximum  $\Delta t$ . The minimum  $\Delta l$  is 2.6  $\mu m$ , the lateral resolution of our OR-PAM system. To avoid phase ambiguity, the maximum measurable  $\Delta t$  is 167 ms, the average time duration between two adjacent cardiac pulses. Thus, a PWV as low as  $1.6 \times 10^{-3}$  cm/s can be measured.

According to known physiology, the PWV is roughly linearly proportional to the vessel diameter in normal physiological conditions.<sup>5,11</sup> As a validation, we measured the PWVs in ten arterial/arteriolar vessel segments, with various diameters, from two nude mice (Hsd:ATHymic Nude-Foxn1NU, Harlan) of the same

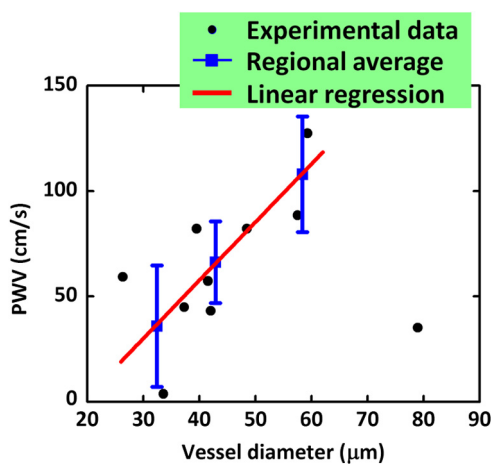


**Fig. 4** Pulse wave velocity versus vessel diameter, measured in ten vessel segments from two mice. The measurements were divided into four categories: 26–38  $\mu\text{m}$ , 38–50  $\mu\text{m}$ , 50–62  $\mu\text{m}$ , and  $> 62 \mu\text{m}$ . The PWV and vessel diameter averaged within each of the first three categories show a linear relationship with an  $r$ -value of 0.999 and a  $p$ -value of 0.012.

batch. Figure 4 shows the experimentally measured PWV versus the vessel diameter. A linear correlation between the PWV and the vessel diameter was observed, with an  $r$ -value of 0.999 and a  $p$ -value of 0.012. The slope of the linear regression was 2.77, which agreed with the values reported in the literature.<sup>5,11</sup> For vessels larger than 80  $\mu\text{m}$  in diameter, our present method failed to give a reasonable estimation of the PWV. The error is likely caused by the inadequate temporal resolution in resolving the short travel time due to a high PWV. Also, fluctuation in the ECG frequency, when measuring at the starting and ending points of the chosen travel path, contributes to inaccuracy.

In conclusion, we have demonstrated, for the first time, an ECG-synchronized photoacoustic method for noninvasive measurements of the PWV in mouse peripheral microvessels. Strong correlations between the simultaneously recorded ECG and the blood flow patterns were observed in arteries and arterioles, but not in veins and venules. Furthermore, a linear relationship between PWV and vessel diameter was observed experimentally, which is in good agreement with the data in the literature.<sup>5,11</sup>

Complementary to ultrasonic measurements of PWV in the aorta, OR-PAM is capable of measuring the PWV in peripheral microvessels. According to the Moens–Korteweg equation,<sup>2</sup> PWV is closely associated with vascular stiffness, vessel wall thickness, and blood density. This innovation holds the potential to study a broad range of peripheral cardiovascular diseases, including diabetes and hypertension, by providing a metric of local vascular stiffness and blood pressure.<sup>2</sup> Extending this method to intravascular photoacoustic endoscopy<sup>12</sup> can

potentially enable early diagnosis of arteriosclerosis.<sup>13</sup> Furthermore, combining PWV with previously quantified vascular anatomy,  $\text{SO}_2$ , blood flow, and the metabolic rate of oxygen,<sup>14</sup> can provide a comprehensive characterization of cardiovascular diseases.

### Acknowledgments

The authors appreciate the close reading of the manuscript by Professors. James Ballard, Seema Dahlheimer, and Lynnea Brumbaugh. Thanks to Amy Winkler and Brian Soetikno for helpful discussions. Thanks to Di Lang for experimental assistance. This work was sponsored by National Institutes of Health Grants R01 EB000712, R01 EB008085, R01 CA134539, U54 CA136398, R01 CA157277, and R01 CA159959. L.V.W. has financial interests in Microphotoacoustics, Inc. and Endra, Inc., which, however, did not support this work. K. Maslov has a financial interest in Microphotoacoustics, Inc.

### References

1. A. K. Reddy et al., “Multichannel pulsed Doppler signal processing for vascular measurements in mice,” *Ultrasound Med. Biol.* **35**(12), 2042–2054 (2009).
2. W. W. Nichols, M. F. O’Rourke, and C. Vlachopoulos, *McDonald’s Blood Flow in Arteries: Theoretical, Experimental and Clinical Principles*, Oxford University Press, Oxford, UK (2011).
3. E. G. Lakatta et al., “Human aging: changes in structure and function,” *J. Am. Coll. Cardiol.* **10**(2, Suppl. 1), 42A–47A (1987).
4. E. Okada et al., “Spectrum analysis of fluctuations of RBC velocity in microvessels by using microscopic laser Doppler velocimetry,” in *Proc. Ann. Int. IEEE EMBS*, Seattle, WA, USA, pp. 1741–1743 (1989).
5. J. Seki, “Flow pulsation and network structure in mesenteric microvasculature of rats,” *Am. J. Physiol.* **266**(2), H811–H821 (1994).
6. J. Yao et al., “In vivo photoacoustic imaging of transverse blood flow by using Doppler broadening of bandwidth,” *Opt. Lett.* **35**(9), 1419–1421 (2010).
7. S. Hu, K. Maslov, and L. V. Wang, “Second-generation optical-resolution photoacoustic microscopy with improved sensitivity and speed,” *Opt. Lett.* **36**(7), 1134–1136 (2011).
8. R. E. Klabunde, *Cardiovascular Physiology Concepts*, Lippincott Williams & Wilkins, Philadelphia, USA (2011).
9. C. J. Hartley et al., “Noninvasive determination of pulse-wave velocity in mice,” *Am. J. Physiol.* **273**(1), H494–H500 (1997).
10. S. Oladipupo et al., “VEGF is essential for hypoxia-inducible factor-mediated neovascularization but dispensable for endothelial sprouting,” *Proc. Natl. Acad. Sci. USA* **108**(32), 13264–13269 (2011).
11. E. Okada et al., “Application of microscopic laser Doppler velocimeter for analysis of arterial pulse wave in microcirculation,” in *Proc. Ann. Int. IEEE EMBS*, Orlando, FL, USA, pp. 564–566 (1990).
12. J.-M. Yang et al., “Simultaneous functional photoacoustic and ultrasonic endoscopy of internal organs in vivo,” *Nat. Med.* (in press).
13. N. Chubachi et al., “Measurement of local pulse wave velocity in arteriosclerosis by ultrasonic Doppler method,” in *Proc. IEEE Ultrason. Symp.*, Cannes, France, Vol. **3**, pp. 1747–1750 (1994).
14. L. V. Wang and S. Hu, “Photoacoustic tomography: in vivo imaging from organelles to organs,” *Science* **335**(6075), 1458–1462 (2012).